Raman scattering from vibrational and magnetic modes in Dy, Er, and Y films

R. T. Demers,* S. Kong, M. V. Klein, R. Du, and C. P. Flynn
Department of Physics, University of Illinois at Urbana-Champaign, 1110 West Green Street, Urbana, Illinois 61801 and Materials Research Laboratory, University of Illinois at Urbana-Champaign, 104 South Goodwin Avenue, Urbana, Illinois 61801
(Received 29 July 1988)

Inelastic-light-scattering spectra were measured in molecular-beam-epitaxy–grown single-crystal films of dysprosium, erbium, and yttrium. Polarized Raman scattering was used to probe vibrational and electronic excitations in Dy, Er, and Y, and magnetic excitations in Dy. The vibrational light-scattering measurements have revealed an anomalous temperature dependence of the Brillouin-zone-center transverse-optical (TO) phonon in Dy and R. Previous measurements of the thermal expansion of bulk Dy and Er indicate that this temperature dependence cannot be explained by lattice anharmonicity and the related volume change. The hardening of this mode may be due in part to the coupling of the TO phonon to the ordered magnetic moments. The ferromagnetic acoustic-spin-wave gap in Dy was observed. The light-scattering measurement of the spin-wave gap energy agrees with and corroborates earlier infrared resonance measurements in bulk Dy. The observation of the optical spin wave in ferromagnetic Dy is forbidden by Raman selection rules. The optical spin wave in spiral-phase Dy was not observed. A broad low-intensity peak centered at about zero energy shift was observed in Er, Dy, and Y films and in bulk Zn. This may be due to interband electronic scattering or two-phonon scattering. The LO phonon was observed in Dy, Er, and Y due to weak disorder.

I. INTRODUCTION

The extraordinary ordered magnetic structures in the heavy rare-earth (HRE) metals led to extensive investigations in the past two decades and the ability to grow coherent modulated structures has stimulated more recent experimental work on the HRE metals.[1] We report in this article the results of a light-scattering investigation of molecular-beam-epitaxy (MBE) –grown single-crystal films of Dy, Er, and Y. This work was motivated by the recent discovery of coherent magnetic order in Dy/Y superlattices[2] and the absence of reported results of light-scattering studies of elemental HRE metals. The understanding of the elemental metals obtained from this work can be used as a foundation for Raman investigations of modulated structures of the HRE metals.

The novel magnetic properties of the HR metals are mainly due to the behavior of the partially filled $4f$-electron shells. The $4f$ electrons interact with the other ions in the crystal through the crystal-field and the exchange interactions. The crystal-field splits the J multiplet levels although the energy of this splitting is much less than the spin-orbit splitting, Δ_0.

The HRE metals (except for ytterbium) crystallize in the hexagonal close-packed (hcp) structure. The space group of the hcp lattice is D^4_{6h} ($P6_3/mmc$). For phonons propagating along the **c** direction the transverse-optic and -acoustic modes are each doubly degenerate. The only measurements of vibrational frequencies in HRE metals are inelastic neutron scattering studies of yttrium,[3] terbium,[4] and limited data on dysprosium[5] and holmium[6]. The zone-center optical modes in Dy have not been measured. Houmann and co-workers measured the phonon dispersion curve of Tb by inelastic neutron scattering.[4] They fit their data to a Born–von Kramann force-constant model including interactions out to the eighth neighbor. The fitted force constants were large out to the fourth neighbors and showed a strong dependence on both intersublattice and intrasublattice bonds. Sinha *et al.* measured phonon-dispersion relations in bulk yttrium using inelastic neutron scattering.[3] They determined force constants using a modified axially symmetric force-constant model to the sixth-nearest neighbors. The Brillouin-zone-center optical models are rigid translations of each sublattice which are 180° out of phase. Thus for these modes the force constants depend only on the intersublattice bonds.

Bulk Dy has two low-temperature ordered magnetic phases. It is paramagnetic from room temperature to about 178.5 K, the Néel temperature, at which point the localized moments order in an antiferromagnetic helix. The moments in this phase are believed to be well described by the following model:

$$\mu_{nx}=\mu\cos(\mathbf{Q}\cdot\mathbf{R}_n+\alpha)\ ,$$

$$\mu_{ny}=\mu\sin(\mathbf{Q}\cdot\mathbf{R}_n+\alpha)\ ,$$

$$\mu_{nz}=0\ ,$$

where μ is the magnitude of the local moment, $\mathbf{R}_n$ is the position vector of the nth moment in the crystal, α is a phase constant determined by anisotropy, and $\mathbf{Q}=(2\pi/\lambda)\hat{\mathbf{z}}$ is the wave vector of the helix, parallel to the c axis of the crystal. Thus all the moments in a single atomic layer in the basal plane are parallel. At a temperature of about 85 K, the Curie temperature, bulk Dy un-

dergoes a first-order phase transition from an ordered helix to a ferromagnet in which all the moments in a single domain of the crystal are parallel and confined to the basal plane:

$$\mu_{nx}=\mu\cos\alpha\ ,$$

$$\mu_{ny}=\mu\sin\alpha\ ,$$

$$\mu_{nz}=0\ .$$

In the ferromagnetic phase all the moments point along one of six equivalent a-axis directions.

The turn angle (and wavelength) in Dy varies continuously from 43.2°/atomic layer ($\lambda=4.17c$) at the Néel temperature to 26.5°/atomic layer ($\lambda=6.79c$) at the Curie temperature. The helical wavelength takes on many values which are incommensurate with the c-axis lattice spacing. At the Curie temperature the turn angle (wavelength) changes discontinuously from 26.5° ($\lambda=6.79c$) to 0° ($\lambda=\infty$). The discontinuity is due to the fact that there are competing terms in the free-energy expansion, each of which dominate in different temperature regimes. The magnetostriction energy favors ferromagnetic ordering accompanied by an orthorhombic lattice distortion at low temperatures while the isotropic exchange energy favors helical ordering in the hcp structure. The contribution of each of these terms to the free energy is temperature dependent and the competition between them determines the temperature of the first-order transition (the Curie temperature) from helical order to ferromagnetic order. The HRE metals exhibit the largest measured magnetostriction.[7] The magnetically ordered moments of Dy are schematically depicted in Fig. 1(a).

The magnetic phases of bulk Er (Ref. 8) are more complex than those of Dy. In the high-temperature ordered magnetic phase of bulk Er (52.4 K $< T <$ 84.4 K) the moments point along the c-axis direction, and they are sinusoidally modulated along the c axis. In the intermediate temperature range (18 K $< T <$ 52.4 K) a basal-plane helix is superimposed on the c-axis modulation (CAM) with the same periodicity and phase. Below the Curie temperature, 18 K, the component of the magnetic moments along the c axis is fixed while the basal-plane moments form a helix whose periodicity is constant with temperature. The latter phase is referred to as a conical ferromagnetic ordering. The three magnetic phases of Er are schematically depicted in Fig. 1(b).

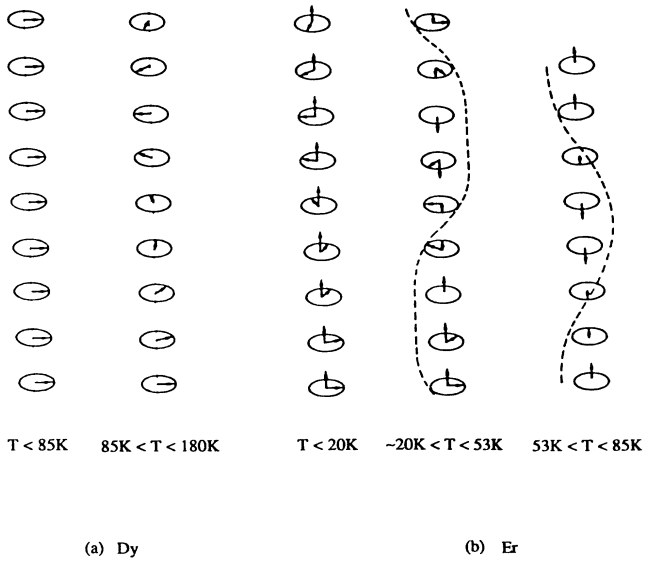

FIG. 1. Schematic of the ordered magnetic phases of (a) dysprosium and (b) erbrium.

There are conflicting experimental results on the variation of the magnetic wave vector with temperature in Er.[9] Cable and co-workers found that at temperatures slightly above 20 K the CAM approaches, but never achieves, a "squared" configuration in which four c-axis moments pointing along the $+\hat{\mathbf{z}}$ direction are followed by four moments pointing along the $-\hat{\mathbf{z}}$ direction. Below 20 K they found the helical turn angle to be constant at 44.0°.

Habenschuss *et al.*[10] found that the turn angle decreases monotonically from 52.38° at 52.4 K to 45.00° at 24 K, which is commensurate with the lattice. They found that the squared configuration remains down to the Curie temperature of 18 K.

II. RAMAN SCATTERING

A. Phonons

The two atoms in the unit cell occupy sites of symmetry D_{3h} ($6m2$). The six normal modes of zero wave vector belong to the irreducible representations

$$A_{2u}+B_{1g}+E_{1u}+E_{2g}\ .$$

For phonons propagating along the c direction the A_{2u} and doubly degenerate E_{1u} modes correspond to the longitudinal- and transverse-acoustic modes, respectively. The B_{1g} and E_{2g} modes are the longitudinal- and transverse-optical modes, respectively. The TO phonon is a shear mode corresponding to the beating of the two hcp sublattices against each other in two orthogonal directions in the basal plane. The E_{2g} mode is Raman active; the B_{1g} mode is silent. The Raman tensor for the doubly degenerate E_{2g} mode contributes to the scattered-light intensity when the polarization of the exciting light is parallel or perpendicular to the scattered-light polarization and these polarizations are in the crystallographic x or y directions.[11]

B. Spin waves

The scattering of light from spin waves always involves the coupling of the electric-field vector of the radiation to the electronic susceptibility of the magnetic system (the electric-dipole coupling).[12] Most of the magnetic materials investigated to date exhibit spin waves which scatter light by an indirect electric-dipole interaction mechanism. This is a third-order process analogous to that for vibrational scattering in which the electronic spin-orbit coupling takes the place of the electron-phonon coupling. Magnons being a linear superposition of the excitations of individual ions from their ground state to their

lowest-lying states, the mechanism of light scattering can be understood in terms of a single-ion excitation. Many magnetic materials (e.g., MnF_2, FeF_2, Fe_2O_3) have an ionic ground state in which the orbital angular momentum is either zero or quenched[13] ($L=0$). The ground multiplet is thus a set of $(2S+1)$ states whose degeneracy is broken by the crystal-field and exchange interaction. The magnon corresponds to the transition from the $S_z=S$ state to the $S_z=S-1$ state. The incident radiation induces an electronic transition from the ground state to a virtual intermediate state which has the same spin S but finite orbital angular momentum L. The ion subsequently relaxes to the lowest possible excited state in the ground multiplet. The total angular momentum J in the intermediate state is a superposition of different $|L_z,S_z\rangle$ states due to the spin-orbit interaction. Although neither of the electric dipole transitions alone changes the ionic spin S_z, the spin-orbit coupling allows a change in S_z in the intermediate state. The electric-dipole operator can alter **L** but not **S**, and therefore spin-orbit coupling is necessary for light scattering from magnons in this case. The spin-wave scattering cross section for this mechanism resembles that of phonons with the electron-phonon interaction being replaced by the spin-orbit interaction[14] and with an extra factor of $\zeta/(E_I-E_0)$, where ζ is the spin-orbit coupling constant and E_I-E_0 is the excitation energy. This mechanism accounts very well for the Raman intensities observed in transition-metal compounds[11] such as MnF_2 and FeF_2.

In the HRE metals, however, the ground-state multiplet has finite orbital angular momentum ($L=5$ in Dy) and the physics is more complex. The light-scattering process does not require spin-orbit coupling in this case because the lowest excited state in the ground-state multiplet has some S_z states in common with the ground state. Another scattering mechanism becomes possible in this case in which the incident light interacts directly with the magnetic excitations. The electric field of the light couples to the orbital part of the magnetic excitations and induces two dipole transitions in which the orbital angular momentum is changed. Ishikawa and Moriya[15] calculated the electric polarizability for both of the mechanisms of magnetic scattering in CoF_2 which has unquenched orbital angular momentum in the ground state. They found that the S-dependent terms of the polarizability are smaller than the L-dependent terms by a factor of $\zeta/(E_I-E_0-\hbar\omega_L)$, where $\hbar\omega_L$ is the laser photon energy. For the HRE metals this factor is about 0.1.

The selection rules for spin-wave excitations are similar to those for phonons, but one has to consider the alteration of the symmetry of the crystal due to the presence of the ordered moments. A localized magnetic moment transforms as an axial vector which is invariant under inversion. In order to invert the spins it is necessary to use the time-reversal operator. The point group of a crystal with ordered magnetic moments includes antiunitary operations, which are products of the time-reversal operator and a rotation, reflection, or inversion, as well as the normal unitary operations (no time reversal). In a magnetic point group half of the operations are unitary and half are antiunitary. The unitary operations taken together form an invariant subgroup of the magnetic point group. There are a total of 58 so-called black and white Shubnikov point groups, and they are listed in standard group-theory texts.[16,17] The Raman susceptibility tensors for the 58 magnetic point groups have been calculated and tabulated by Cracknell.[18]

In order to determine the symmetry of the acoustic and optic magnons in ferromagnetic Dy we refer to Fig. 2 which shows a schematic diagram of the classical interpretation of the zone-center spin-wave modes in Dy. The two ions per unit cell lead to two spin-wave modes. The acoustic mode is an in-phase oscillation in the basal plane of the two moments. This angular displacement transforms as a rotation about the x axis (i.e., the R_x or yz operator) which belongs to the DB_g representation of the D_{2h} ($m'm'm$) point group or the B_g representation of the C_{2h} point group. The optical mode is an oscillation in the plane in which the two moments are 180° out of phase, resulting in a net oscillating moment along the z direction. This oscillation transforms as the z coordinate which belongs to the DA_u representation of the D_{2h} ($m'm'm$) point group or the A_u representation of the C_{2h} point group. The acoustic magnon is thus Raman active, while the optical magnon is inactive.

According to Cracknell[18] the symmetry restricted form of the susceptibility tensors for D_{2h} ($m'm'm$) are

$$DA_g: \begin{bmatrix} A & iB & 0 \\ iD & E & 0 \\ 0 & 0 & I \end{bmatrix}, \quad DB_g: \begin{bmatrix} 0 & 0 & iC \\ 0 & 0 & F \\ iG & H & 0 \end{bmatrix}.$$

For magnon scattering in crystals whose ionic ground state has zero orbital angular momentum the susceptibility tensors are required to be antisymmetric. This is analogous to the symmetric tensor requirement of vibrational scattering. This rule does not apply in our case. The above susceptibility tensors have an antisymmetric part and a symmetric part due to the mixed orbital and spin nature of the ionic ground state. The result is that acoustic spin-wave scattering is allowed in two general

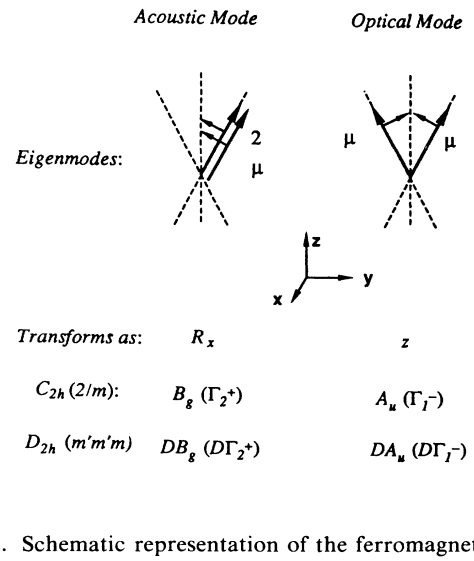

FIG. 2. Schematic representation of the ferromagnetic spin-wave eigenmodes and their symmetries.

scattering geometries: one in which the incident and scattered light polarizations are parallel and one in which the polarizations are perpendicular. The resulting intensities for these two scattering geometries are[19] [Eqs. (37) and (38) of Ref. 19, respectively]

$$\langle I_{\parallel}(DB_g)\rangle_\theta = \tfrac{1}{8}|H|^2 + \tfrac{1}{8}|F|^2 + \tfrac{1}{8}(H^*F + HF^*) ,$$

$$\langle I_{\perp}(DB_g)\rangle_\theta = \tfrac{1}{8}|H|^2 + \tfrac{1}{8}|F|^2 - \tfrac{1}{8}(H^*F + HF^*) ,$$

where the angular brackets represent an average over the angle between the polarization vector of the incident light and the y axis.

III. EXPERIMENT

The samples investigated in this work were grown specifically for light-scattering experiments. A custom built molecular-beam-epitaxy chamber with an e-beam source was used to grow (110) Nb on (11$\bar{2}$0) sapphire (Al_2O_3). hcp Y crystals of very high quality can be grown along the [0001] direction on the (110) surface of Nb. The sample growth details have been described elsewhere.[2] A typical Dy film grown for Raman measurements included 500–800 Å of (110) Nb grown on a 0.5-cm^2 square of sapphire. About 300 Å of (0001) Y was then grown on the Nb to serve as a buffer between the substrate and the (0001) Dy (or other HRE). The Dy film thickness fell in the range between 5000 and 6500 Å. The Dy and Er films grown for Raman measurements included a 40-Å surface "cap layer" of (0001) Y to retard the contamination of the surface by atmospheric oxygen. The Y films had a Nb substrate layer similar to that of the Dy films and an outer Y layer of about 5000 Å. When samples were not being used for optical measurements they were stored under vacuum in a dessicator as an additional measure to retard oxidation.

All films were characterized by *in situ* reflection high-energy electron diffraction during the growth process. All films were found to have atomically smooth surfaces. Several of the films grown for light scattering were characterized by x-ray diffraction using a Rigaku D-max diffractometer. The c axis lattice parameters obtained from 2θ scans were found to be close to those of bulk crystals. The (0002) peaks had typical rocking curve widths of 0.20°. The best rocking curve widths belonged to the Y films which were as low as 0.15°.

Dy films previously grown with thicknesses greater than 5000 Å exhibited the spiral and ferromagnetic phases in zero field with Néel and Curie temperatures within ~8 K of those of bulk single crystals.[20] Moreover, Hong *et al.*[21] carried out a systematic study of the dependence of Dy magnetic properties on film thickness. They found that films of thickness 5000 Å or greater had the same Curie temperature as bulk Dy, whereas reducing the film thickness depressed the Curie temperature. 200-Å-thick films had a transition temperature of 25 K and 76-Å-thick films had the ferromagnetic phase completely suppressed. The suppression of the ferromagnetic phase in thin films is due to the fact that the atomic layers of Dy in the vicinity of the Y substrate cannot undergo the magnetostrictive orthorhombic distortion which makes the transition energetically more favorable. Thick films, however, have enough strain relief to allow the layers near the surface to behave like the bulk material.

By contrast, we found Er films to have no ferromagnetic ordering even with thicknesses as large as 9000 Å.[2] The Er films do have the c-axis modulation and the basal-plane spiral phases This behavior is not yet understood.

Raman spectra were excited by 5145-Å or 4880-Å light from an argon-ion laser. The experiments on metals were always conducted in the "pseudo-backscattering" geometry in which the exciting light is incident on a reflecting surface at an acute angle with respect to the surface normal and the scattered light which is propagating in a direction parallel to the normal is detected. The index of refraction of opaque materials is generally large enough to refract the incident light so that it is propagating in a direction nearly parallel to the surface normal in the crystal.

The linearly polarized laser light was focused on the sample at an angle of incidence of about 70°, close to the pseudo-Brewster's angle, in order to maximize the transmission efficiency. The laser light power was typically 500 mW. Two crossed cylindrical lenses were used to focus the light on the sample surface. The scattered light was collected along a direction normal to the film surface and was analyzed by a low-reflectivity polarizing cube. A half-wave plate was used to rotate the polarization parallel to the grating grooves for maximum efficiency.

To provide adequate stray light rejection a homemade "third" single-grating monochromator (500-mm focal length) was added to an existing Spex double-grating monochromator (850-mm focal length). The three gratings were oriented and scanned for additive dispersion. In many spectra weak, but sharp, lines appeared which were fluorescences of the argon-ion plasma reflected by the sample surface into the monochromator. The frequencies of these plasma lines (relative to the 5145-Å lasing line) are 66, 77, 117, and 267 cm^{-1}.

The sample was mounted on the bottom of the inset of a Janis model 8-DT Varitemp liquid-helium cryostat. The sample was cooled to as low as ~20 K with flowing cold Helium gas. When temperatures as low as 2 K were necessary, the sample was either immersed or in "cold-finger" contact with superfluid liquid helium. Temperature stability was maintained using a Lake Shore Cryotronics model DRC 80C temperature controller with a silicon diode thermometer and a 120-Ω coil heater both located within 2 cm of the sample. The sample temperature was determined from the measured inelastic-phonon peak intensities and the temperature-dependent relation between the Stokes and anti-Stokes intensities.

IV. RESULTS AND DISCUSSION

A. Vibrational modes

In the backscattering geometry the polarizations of the exciting and scattered light were always in the hcp basal plane since all films in this investigation were grown

along the c axis. The TO phonon is allowed in $z(xx)z$ and $z(xy)z$ geometries with equal intensities. As shown in Fig. 3 we observed the TO phonon in Dy in both of these geometries with equal peak intensities and line widths. The same result was observed in Y and Er. The room-temperature frequencies of this mode in Y, Dy, and Er are 88.5, 63.0, and 66.5 cm^{-1}, respectively. Our measurement of the Y TO frequency is in close agreement with the value 89.5 cm^{-1} determined by the inelastic neutron scattering measurement of Sinha *et al.*[3] No earlier measurements of this mode in Dy and Er have been reported. The much larger frequency of the Y mode is expected in view of the much smaller mass of Y. Indeed the ratio of the TO mode frequencies of Dy and Y is 0.712 and the inverse ratio of the square roots of their atomic masses is 0.740, a difference of $\sim 4\%$. This comparison implies that to zeroth order the force constants depend only weakly on the ionic species. The 5% difference between the frequencies of Dy and Er is less transparent. The 3% larger ionic mass of Er would tend to decrease the mode frequency relative to Dy, while the 3% smaller unit-cell volume of Er would tend to increase the frequency. The two extra electrons of Er are $4f$ electrons which do not interact strongly with the conduction band and have very little mutual overlap and are thus not expected to have much of an effect on the force constants.

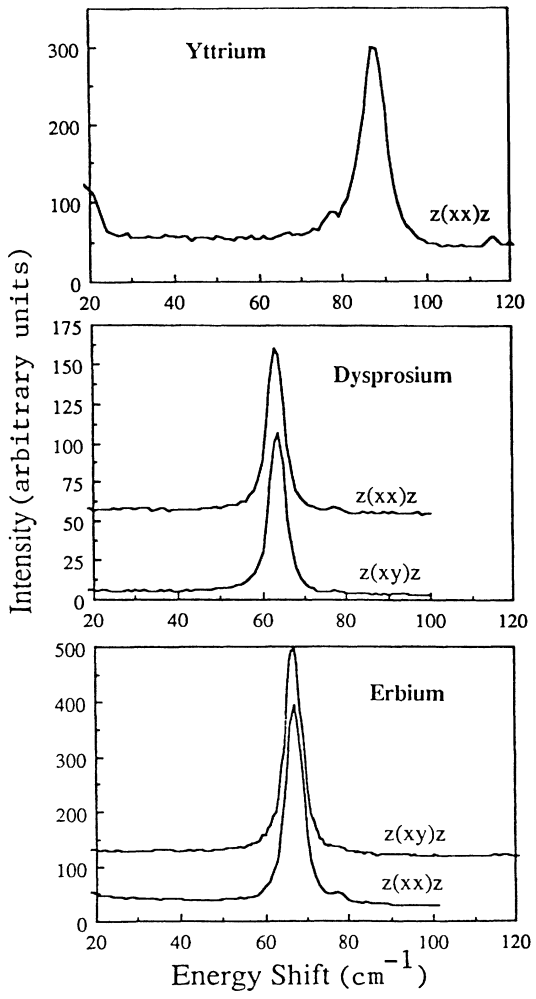

FIG. 3. Raman spectrum of the TO phonon in Y, Dy, and Er.

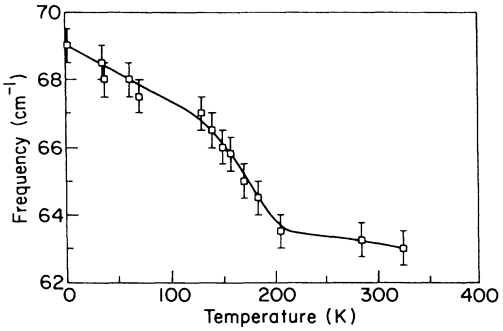

FIG. 4. Temperature dependence of the TO-phonon frequency in Dy. The solid line is a guide to the eye.

The temperature dependence of the TO phonon in Dy, Er, and Y was measured and the results are plotted in Figs. 4, 5, and 6. The temperature dependence of the linewidths of this mode in Dy and Er is shown in Figs. 7 and 8. The Dy TO-mode frequency hardens from 63 to 69 cm^{-1} (a change of about 10%) as temperature is lowered from 330 to 2 K. The Er TO-mode frequency hardens from 66.5 cm^{-1} at 340 K to 75 cm^{-1} at 2 K (a 13% frequency shift). The temperature dependence of the TO mode frequency in both Dy and Er is anomalous because of an apparent change of the slope in low-temperature regimes. This behavior is more easily understood in Dy since the Dy films behave like bulk crystals.

At high temperatures the TO mode in Dy hardens relatively slowly with temperature. The slope changes discontinuously at about 200 K to a larger (negative) value. This slope is constant until about 125 K where the slope changes discontinuously again to a smaller (negative) value. The temperature region $125\ \text{K} < T < 200\ \text{K}$ corresponds roughly to the magnetic helical phase in which the magnetic ordering is continuously varying with temperature. Above the Néel temperature (180 K) there is no magnetic ordering and below the Curie temperature (85 K) the ordering is ferromagnetic and does not vary with temperature. The temperature dependence of the phonon frequency thus hints at a coupling of the phonon

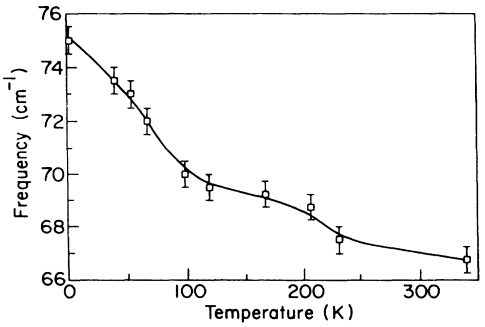

FIG. 5. Temperature dependence of the TO-phonon frequency in Er. The solid line is a guide to the eye.

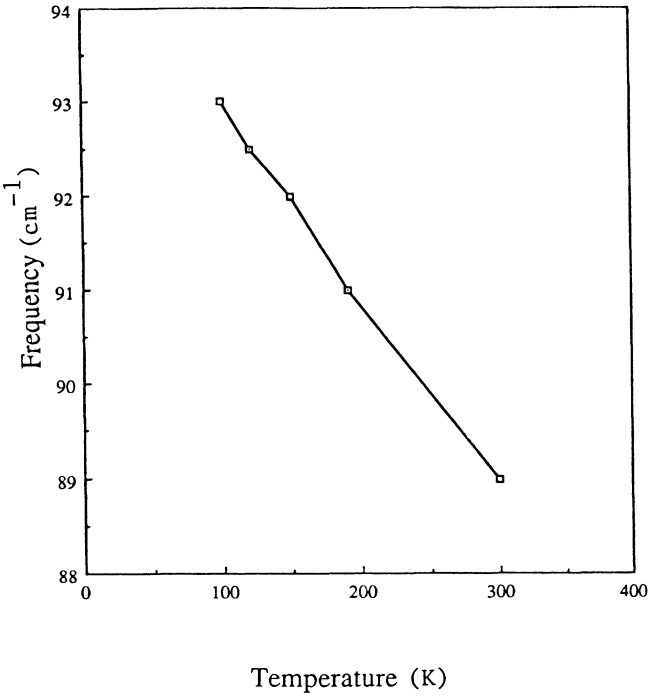

FIG. 6. Temperature dependence of the TO-phonon frequency in Y. The solid line is a guide o the eye.

to the magnetization.

One might try to explain this behavior in terms of anharmonicity of the ionic interaction energy. In a crystal with significant anharmonic terms in the lattice potential, the normal mode frequencies depend on the equilibrium positions of the ions. Thus anharmonicity results in a coupling of the strain terms to the force constants. Schulz and Hüfner[22] measured a smooth temperature dependence of the TO mode in Zn, another hcp metal, and ascribed the hardening to anharmonicity. They successfully fitted their data to a theory which explicitly included the anharmonicity of the lattice potential. The anharmonicity contributes to the phonon linewidth by activating a two-phonon decay process which vanishes at low temperatures.

In Dy and Er the changes in the lattice constants are caused not only by the thermal expansion due to anharmonicity but also by the unusually large magnetostriction. The change in the Dy lattice constants with temperature in zero magnetic field were measured by Clark *et al.*[23] and by Rhyne[24] using a strain-gauge method. Above 180 K when Dy is paramagnetic, the lattice contraction resembles the normal anharmonic thermal behavior. Below 180 K the *a*- and *b*-axis lattice constants continue to decrease as the temperature is lowered. The identical behavior in both lattice directions is an indication of basal plane isotropy. The *c* axis, however, shows the opposite behavior below 180 K, namely increasing as temperature is lowered. All three lattice constants show anomalies at the Néel and Curie temperatures. The slopes change discontinuously at the Néel temperature and in zero field the lattice constants are discontinuous at the Curie temperature due to the first-order transition to an orthorhombic structure with ferromagnetic order.

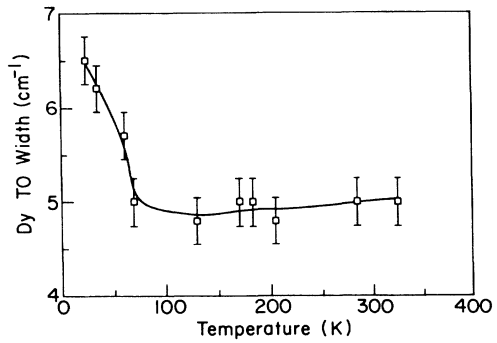

FIG. 7. Temperature-dependent TO-phonon linewidth in Dy. The solid line is a guide to the eye.

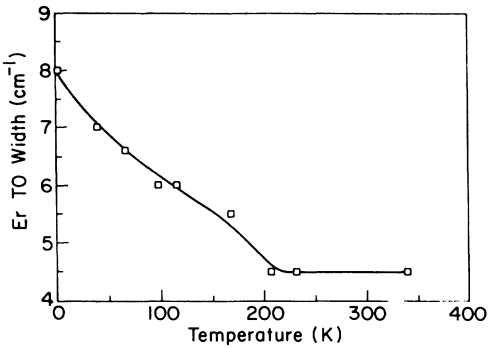

FIG. 8. Temperature-dependent TO-phonon linewidth in Er. The solid line is a guide to the eye.

From the results of Clark *et al.* we have calculated the total fractional change in the unit cell volume for the paramagnetic and helical phases and from the Raman data we determined the corresponding shifts in the TO-mode frequency. The results appear in Table I. As the table shows, the fractional volume change in the helical phase is an order of magnitude smaller than that of the paramagnetic phase. This is due to the fact that the *c*-axis expansion compensates to some extent for the *a*- and *b*-axis contraction in the helical phase. The TO phonon energy, however, shifts twice as much in the helical phase as the paramagnetic phase. The simplest phenomenological theories of anharmonic mode hardening predict an increase of the mode frequency as the unit-cell volume decreases.[25] In this case such a description would be inadequate since the phonon hardens most in the temperature regime where the unit-cell volume changes least. Moreover the phonon-frequency hardening is monotonic with temperature. It follows the basal-plane contraction rather than the *c*-axis expansion since the *c*-axis temperature dependence is not monotonic. The $\mathbf{q}=0$ TO-phonon energy depends only on the intersublattice force constants. If the mode hardening were due only to anharmonicity it follows that the TO-mode frequency would have to depend primarily on those intersublattice force constants between ions whose bonding direction is very nearly parallel to the basal plane. This is highly unlikely given

TABLE I. Net changes in unit-cell volume and TO-mode frequency in the paramagnetic and helical phases of dysprosium.

Temperature range	$\frac{\Delta c}{c}$	$\frac{\Delta a}{a}$	$\frac{\Delta V}{V}$	$\Delta\omega$ (cm^{-1}) (Raman measurement)
180 K $< T <$ 300 K	−0.0014	−0.0007	-2.8×10^{-3}	+1.25
85 K $< T <$ 180 K	+0.0030	−0.0017	-4.0×10^{-4}	+3.0

the force constant models of other HRE metals.[3,4] The largest intersublattice force constants are those between nearest-neighbor ions. The bonding direction of nearest neighbors is at an angle of 54° relative to the basal plane. Thus the anomalous behavior of the TO mode cannot be attributed to anharmonicity.

It is likely that there is another mechanism which is responsible for the phonon hardening. There may be a more direct coupling between the force constants and the localized moments which leads to the anomalous phonon hardening. This could occur by a mechanism involving the conduction electrons as intermediary. The force constants depend on the conduction band which is perturbed by the localized moments through the *s-f* exchange interaction between the 4*f* electrons and the conduction electrons. The continuous and monotonic variation of the helix periodicity with temperature would explain the similar variation of the phonon frequency in the helical phase. As the helical periodicity changes so does the perturbation of the conduction-electron levels.

Another possible mechanism is the addition of the magnetoelastic terms to the nonmagnetic elastic energy terms. This additional strain-dependent energy is responsible for the anomalous thermal expansion and would also change the energy of small ionic oscillations about their equilibrium positions. A theory of magnetoelastic effects has been applied by Thalmeier and Fulde[26] to explain the splitting in a magnetic field of doubly degenerate optical phonons in paramagnetic $CeCl_3$ observed by Schaack.[27]

We observed a broadening of the TO-phonon linewidth in Dy below ~70 K (Fig. 4). This could be an unresolved splitting of the TO mode due to the orthorhombic distortion in the ferromagnetic phase and would be analogous to a splitting observed by Schaack of a 109 cm^{-1} E_{2g} mode in $CeCl_3$ in a magnetic field in the basal plane.[27] As a result of the lattice transition from hcp to an orthorhombic structure the E_{2g} mode splits into an *A* mode and a *B* mode. Our splitting would be less than 1 cm^{-1}, the limit of our instrumental resolution.

We have observed evidence for magnetoelastic effects by measuring the shift of the TO phonon in Dy caused by a magnetic field applied in the *a-b* plane. Magnetic-field experiments were conducted using the high-field magnet optical setup of the Francis Bitter National Magnet Laboratory at the Massachusetts Institute of Technology. The sample was cooled with helium gas, but the exact temperature of the sample was unknown because this apparatus lacked a thermometer. The TO phonon was observed to harden by 2.5 cm^{-1} as the field was raised to 8 T.

The zero-field hardening of the TO phonon in Er also appears anomalous. It is likely that this effect is also due to magnetic mechanisms; however, it is difficult to strictly apply the above arguments to Er films since the temperature dependence of the lattice constants is not known. Bulk strain-gauge measurements of Er are available[28] but the MBE-grown Er films did not exhibit the ferromagnetic phase, and thus the bulk measurements do not represent the behavior of the films.

B. Spin waves

The Raman spectra of Dy in the two scattering geometries at low temperature appears in Fig. 9. The acoustic magnon was observed in the depolarized spectrum but not in the polarized spectrum. Since the stray light was much greater in the polarized spectrum the magnon may very well be hidden in the intense background. Figure 10 shows the depolarized Raman spectrum in Dy taken at five temperatures in zero magnetic field. These spectra show the expected softening of the magnon energy with temperature. We have measured the magnon energy to be 22 cm^{-1} at 25 K with a full width at half maximum of 6 cm^{-1}. This is in agreement with earlier measurements by infrared resonance[29] and complements the measurements of inelastic neutron scattering.[5] This is the first reported detection of spin waves by Raman scattering in a metal. The difficulty of the measurement is clear from the proximity of the magnon peak to the laser tail and from the peak intensity of about seven counts per second. Sandercock and Wettling[30] have observed magnons in polycrystalline Fe and Ni by

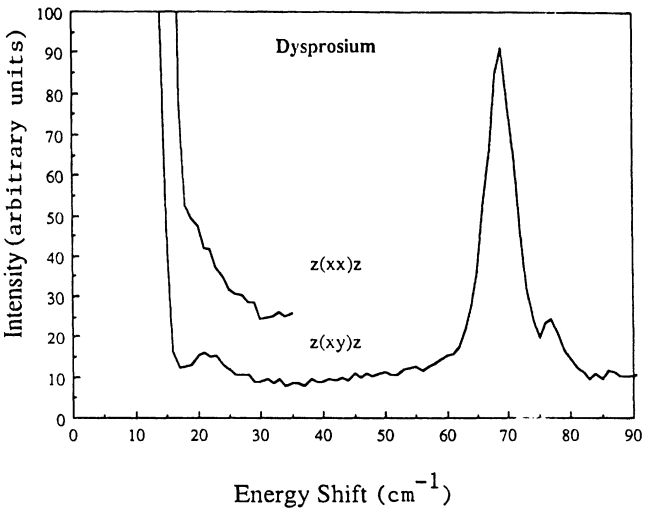

FIG. 9. Spin-wave Raman spectra of Dy in two geometries.

Brillouin scattering in an applied field.

There are three mechanisms by which magnons can decay. They can scatter off of impurities, conduction electrons, and other magnons. At low temperatures the magnon-magnon interactions are expected to be small, whereas at higher temperatures magnon-magnon decay channels are usually significant. Zero wave vector conduction-electron decay channels are unavailable due to the exchange splitting of different sheets of the Fermi surface corresponding to different spin states. A conduction electron can only absorb a magnon whose wave vector is equal to or greater than the wave vector spanning the splitting between the sheets. Thus the width of the zero-wave-vector magnon is a measure of the lifetime limited by impurities and magnon-magnon interactions. At 30 K we measured a relative broadening Γ/ω of about 0.3. Nicklow measured a relative width of the Dy zone-center magnon of about 0.1 at 78 K.[31] This indicates that magnon-magnon interactions have little effect below ~ 80 K in Dy. The fact that we measure a slightly larger width at a lower temperature may be due to impurities. Similar results have been obtained by Møller *et al.*[32,33] in Tb. They found the magnon width to increase rapidly above 100 K (presumably due to two magnon scattering) and the relative width of the zone-center magnon was on the order of 0.1 at 4.2 K.

C. Low-intensity scattering

Figure 11 shows both the Stokes and anti-Stokes Raman spectra of Er and Dy in the parallel-polarization geometry taken at room temperature. A broad peak centered at about zero-energy shift with a full width of ~ 300 cm^{-1} is visible on an intensity scale much smaller than the peak intensity of the TO phonon. Similar broad peaks were observed by us in Y films and bulk samples of Zn. The spectra taken in the perpendicular-polarization geometry exhibit similar, but much weaker peaks. In addition to the broad peak in Y there are weak Stokes and anti-Stokes peaks at 150 cm^{-1} and an asymmetric peak with a cutoff at about 280 cm^{-1}. Similar but somewhat weaker peaks appear in the spectrum of Er at about 120 and 200 cm^{-1}. Figure 12 shows the evolution of the

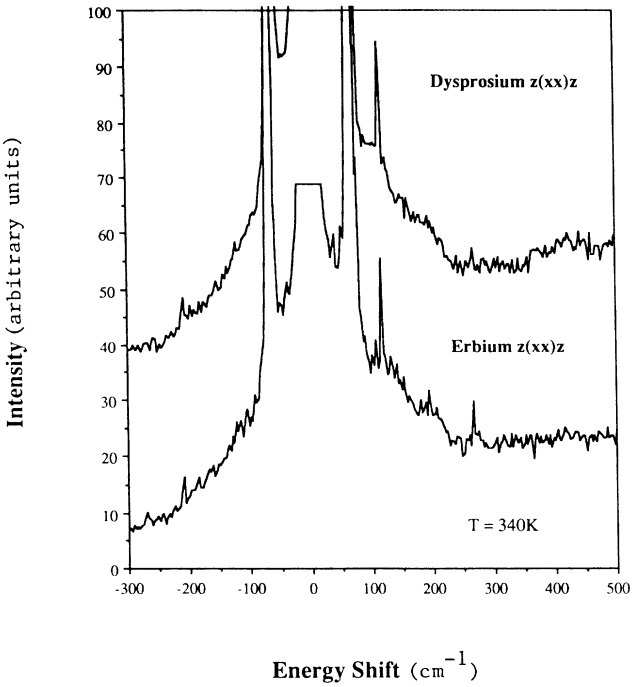

FIG. 11. Raman spectra of Dy and Er at room temperature. The intensity of the Dy spectrum is offset by +30 units.

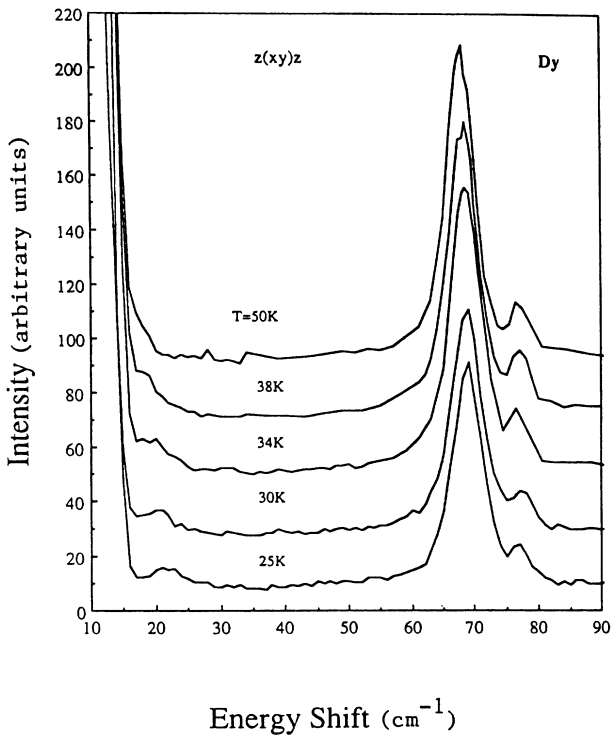

FIG. 10. Crossed-polarization spin-wave spectra of Dy in zero magnetic field as a function of temperature.

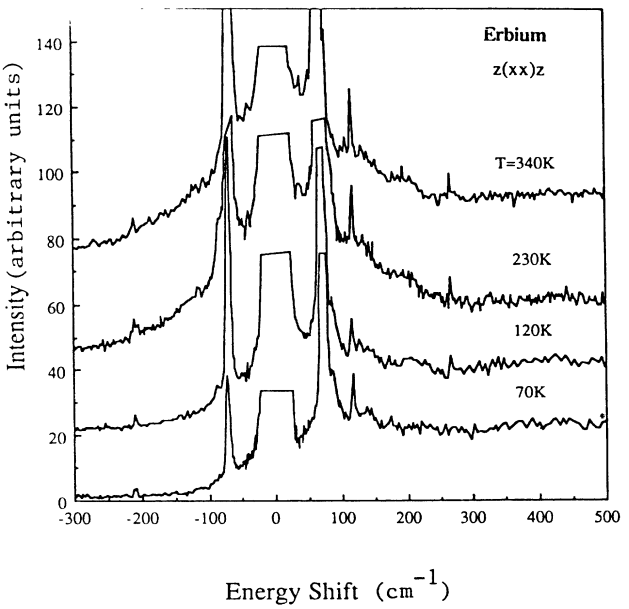

FIG. 12. Raman spectra of Er at various temperatures.

broad peak in Er with temperature. The anti-Stokes tail of the peak is diminished as the temperature is lowered, whereas the Stokes tail shows no change. Below 70 K the anti-Stokes half width is less than 50 cm^{-1}. The linear background in the Stokes scattering has a constant intensity of about 20 counts per second from 300 to 2 K; it extends beyond 1500 cm^{-1} with a gradual rise in intensity. The linear background appears unchanged when an exciting laser wavelength of 4880 Å is used. It exhibits an apparent turn on at zero-energy shift which is independent of the exciting frequency. This behavior is similar to luminescence and has been observed and investigated in the light-scattering spectra of other metals.[34]

It is difficult to determine whether the broad central peak is quasielastic or inelastic. (The term central peak is used here to indicate the close proximity of the peak frequency to the exciting line.) The peak frequency is clearly below 100 cm^{-1}. Phenomenological models used to determine the peak frequency of such a broad peak are usually inconclusive. In order to determine whether there is an intrinsic temperature dependence of the broad peak, the extrinsic temperature-dependent Bose term was factored out of the Er spectra taken at 340 and 70 K. The plotted result is shown in Fig. 13. The linear Stokes background is unaffected but the broad central peak has a much narrower width at low temperature whereas the peak intensity is nearly the same at both temperatures.

Three possible sources for the central peak—intraband electronic scattering, interband electronic scattering, and two-phonon scattering—will now be discussed.

Two-phonon Raman scattering is usually strongest for phonons which show anomalies in their dispersion, such as the phonons of transition-metal compounds.[35] In this case the Raman amplitude is proportional to the modulus of that part of the phonon self-energy which determines the anomalous phonon dispersion. There are, however, no known phonon anomalies in the HRE metals.[3,4] Two-phonon spectra usually exhibit structure in the form of peaks at energies equal to overtones (2ω) of zone-edge acoustic phonons and zone-center optical phonons. The only structure corresponding to overtones is the cutoff at 215 cm^{-1} in Er and Dy (280 cm^{-1} in Y) corresponding to twice the zone-center LO-mode frequency. Furthermore, the greatest intensity of the central peak is at or near zero frequency which corresponds to two-phonon difference scattering. We do not know of any previous case where two-phonon difference scattering is intense while sum scattering is almost unobservable. In any case the peaks at $2\omega_{LO}$ must be ascribed to overtone scattering.

Intraband electronic processes are an unlikely source of the central peak since the intraband scattering intensity in a normal metal[36] is proportional to the frequency shift ω up to a cutoff energy equal to v_f/δ. The scattering intensity in the present case falls off rather than increases from zero shift. Also, v_f/δ in this case has a value of ~ 700 cm^{-1} (assuming a value of 0.5 Ry for the Fermi energy[37]). The Stokes intensity of the central peak in Er at room temperature for example tails off at about 350 cm^{-1}, much lower than v_f/δ. Lastly, if d-electron intraband processes are the dominant mechanism for zero-wave-vector phonon decay, then anomalous dispersion of these phonons occurs and this leads to asymmetric Raman line shapes for optical phonons[38] which we do not observe.

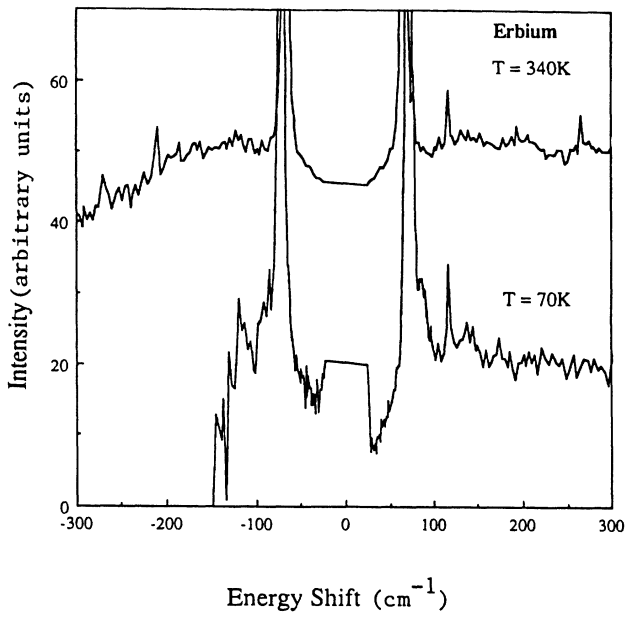

FIG. 13. Raman spectra of Er with intrinsic Bose factor removed.

Interband scattering processes are a possible source of the central peak. The interband scattering mechanism responsible for a broad peak centered at or near zero would have to involve transitions between two bands which cross at an energy close to the Fermi level. The transitions would be vertical since the wave-vector transfer is close to zero. Such a crossing exists in Dy at the L point at an energy less than 0.2 eV above the Fermi energy, according to the band-structure calculation of Keeton and Loucks.[39] According to their calculations near crossings of bands also occur at the K and H points at about 0.5 eV below the Fermi energy. If the interband scattering mechanism involves transitions between the two bands crossing at the L point, then the scattering rate would vanish at low temperatures at which most of these states are unoccupied and thus unavailable for scattering. This would explain the observed intrinsic temperature dependence of the central peak.

The peaks at 120 cm^{-1} in Er and Dy, and 150 cm^{-1} in Y correspond to the LO phonon. The LO mode has not been observed in Er previously but it has been measured by inelastic neutron scattering in Tb (Ref. 4) at 109 cm^{-1} and in Y (Ref. 3) at 155 cm^{-1}. The mechanism for scattering from this silent mode can only be disorder. Lattice disorder breaks the translational symmetry, thus relaxing the requirement of crystal momentum conservation. In order to characterize the disorder, x-ray diffraction measurements were made in samples of Er and Y. The width of the (0002) Er and Y peaks were 0.154° and 0.116°, respectively, a strong indication of order along the c-axis direction. Nonetheless the 2θ scans of both materials have a very weak asymmetric broadening

of the base of the main (0002) peaks. This is an indication of a slight broadening of the distribution of c-axis lattice spacings. This could be caused by some staking faults or by the strain at the interface between the rare earth film and its underlayer. The strain disorder at the interface, however, cannot be responsible for the disorder induced Raman spectra since Raman scattering probes the modulation of the susceptibility by bulk excitations only within the optical penetration depth.

V. CONCLUSIONS

We have used inelastic light scattering to investigate MBE-grown single-crystal films of Dy, Er, and Y. Phonon, magnon, and possibly electronic excitations were observed.

The zone-center TO phonon frequencies Y, Dy, and Er were measured. The temperature dependences of the TO-mode frequencies in Dy and Er were found to be anomalous. Most of the hardening in Dy occurs in the helical magnetic phase. This temperature dependence cannot be explained by common theories of anharmonic ionic interactions. In Dy the slope of the TO-mode frequency versus temperature curve changes precipitously near the Néel and Curie temperatures. This is a strong indication of some sort of direct coupling between the force constants and the ordered magnetic moments. This might occur through (1) a perturbation of the conduction band due to the exchange interaction with the localized $4f$ electrons, or (2) the addition of magnetoelastic terms to the usual strain-dependent elastic energy terms.

The spin-wave energy gap in ferromagnetic Dy was observed for the first time by light scattering. We observe the spin-wave gap in Dy only in the crossed polarization geometry. If it exists in the parallel polarization geometry it is too weak to be observed. Our measurement of the magnon width at low temperatures is close to the widths measured previously by infrared resonance[31] and indicates that magnon-magnon interactions do not have much effect below ~ 80 K. The mechanism of light scattering from the ferromagnetic magnon is in question. Both the spin-orbit coupling and the direct electronic coupling mechanisms are likely to contribute, but one may very well dominate the scattering. Theoretical work and further experimental investigation is required to determine which may be the dominant mechanism. We have shown that light scattering is a significant tool in the measurement of low-frequency metallic spin waves. Light scattering probes true dynamic excitations since the wavelength of the excitation is small compared to the sample dimensions (and large compared to the unit-cell dimensions). Infrared resonance, by contrast, would probe static mode excitations which depend on the sample dimensions since the wavelengths would be larger than the film thickness.

Lastly, we have observed a broad, low-intensity peak centered at about zero energy in Y, Dy and Er. This is probably due to interband electronic scattering or two-phonon scattering. Weak shoulders on this peak are probably caused by overtones of the zone-center LO phonon.

ACKNOWLEDGMENTS

The authors would like to thank J. Borchers for her assistance in characterization of several samples and both J. Borchers and M. B. Salamon for very beneficial discussions. We also thank D. Heiman of the Francis Bitter National Magnet Laboratory for assistance with the field-dependent measurements on Dy. This work was supported by the National Science Foundation (NSF) under Grant Nos. NSF-DMR-80-20250, NSF-DMR-83-16981, NSF-DMR-84-06473, NSF-DMR-85-21616, and NSF-DMR-87-15103. Sample characterization was carried out in the Center for Microanalysis of the Materials Research Laboratory, which is supported by the U.S. Department of Energy under Contract No. DE-AC02-76ER01198.

---

*Present address: Rocketdyne Division, Rockwell International Corporation, 6633 Canoga Avenue, Canoga Park, CA 91303.

[1]See, for example, the collection of review articles in *Magnetic Properties of Rare Earth Metals,* edited by R. J. Elliott (Plenum, London, 1972).

[2]J. Borchers, S. Sinha, M. B. Salamon, R. Du, C. P. Flynn, J. J. Rhyne, and R. Erwin, J. Appl. Phys. **61**, 4049 (1987).

[3]S. K. Sinha, T. O. Brun, L. D. Muhlestein, and J. Sakurai, Phys. Rev. B **1**, 2430 (1970).

[4]J. C. Glyden Houmann and R. M. Nicklow, Phys. Rev. B **1**, 3943 (1970).

[5]R. M. Nicklow and N. Wakabayashi, *17th Magnetism and Magnetic Materials Conference, (Chicago, 1971),* Proceedings of the 17th Annual Conference on Magnetism and Magnetic Materials, AIP Conf. Proc. No. 5, edited by D. C. Graham and J. J. Rhyne (AIP, New York, 1972), p. 1446.

[6]J. A. Leake, V. J. Minckiewicz, and G. Shirane, Solid State Commun. **7**, 535 (1969).

[7]Earl Callen, J. Appl. Phys. **39**, 519 (1968).

[8]W. C. Koehler, in *Magnetic Properties of Rare Earth Metals,* edited by R. J. Elliott (Plenum, London, 1972), p. 81.

[9]B. Coqblin, *The Electronic Structure of Rare-Earth Metals and Alloys: The Magnetic Heavy Rare-Earths* (Academic, New York, 1977), p. 54.

[10]M. Habenschuss, C. Stassis, S. K. Sinha, H. W. Deckman, and F. H. Spedding, Phys. Rev. B **10**, 1020 (1974).

[11]W. Hayes and R. Loudon, *Scattering of Light by Crystals* (Wiley, New York, 1978), p. 37.

[12]P. A. Fleury and R. Loudon, Phys. Rev. **166**, 514 (1968).

[13]D. J. Lockwood, in *Light Scattering in Solids III,* edited by M. Cardona and G. Guntherodt (Springer-Verlag, Berlin, 1972), p. 59.

[14]Y. R. Shen and Bloembergen, Phys. Rev. **143**, 143 (1966).

[15]A. Ishikawa and T. Moriya, J. Phys. Soc. Jpn. **30**, 117 (1971).

[16]G. Burns, *Introduction to Group Theory with Applications* (Academic, New York, 1977).

[17]M. Tinkham, *Group Theory and Quantum Mechanics* (McGraw-Hill, New York, 1964).

[18]A. P. Cracknell, J. Phys. C **2**, 500 (1969).
[19]R. T. Demers, Ph.D. thesis, University of Illinois, 1988.
[20]J. Borchers (private communication).
[21]M. Hong, R. M. Fleming, J. Kwo, L. F. Schneemeyer, J. V. Waszczak, J. P. Mannaerts, C. F. Majkrzak, Doon Gibbs, and J. Bohr, J. Appl. Phys. **61**, 4052 (1987).
[22]H. Schulz and S. Hüfner, Solid State Commun. **20**, 827 (1976).
[23]A. E. Clark, B. F. DeSavage, and R. Bozorth, Phys. Rev. **138**, A216 (1965).
[24]J. J. Rhyne, Ph.D. thesis, Iowa State University, 1965.
[25]A. A. Maradudin and A. E. Fein, Phys. Rev. **128**, 2589 (1962).
[26]P. Thalmeier and P. Fulde, Z. Phys. B **26**, 323 (1977).
[27]G. Schaack, Solid State Commun. **17**, 505 (1975); Z. Phys. B **26**, 49 (1977).
[28]J. J. Rhyne and S. Legvold, Phys. Rev. **140**, A2143 (1965).
[29]H. S. Marsh and A. J. Sievers, J. Appl. Phys. **40**, 1563 (1969); A. J. Sievers, *ibid.* **41**, 980 (1970).
[30]J. R. Sandercock and W. Wettling, J. Appl. Phys. **50**, 7784 (1979).
[31]R. M. Nicklow, J. Appl. Phys. **42**, 1672 (1971).
[32]M. Nielsen, H. B. Møller, and A. R. Mackintosh, J. Appl. Phys. **41**, 1174 (1970).
[33]H. B. Møller and A. R. Mackintosh, J. Phys. (Paris) Colloq. **5**, Suppl. 5, C5-28 (1979).
[34]D. G. Bruns, Ph.D. thesis, University of Illinois, 1979.
[35]M. V. Klein, Phys. Rev. B **24**, 4208 (1981).
[36]M. V. Klein, in *Light Scattering in Solids III*, edited by M. Cardona and G. Güntherodt (Springer-Verlag, Berlin, 1982), p. 121.
[37]K. N. Taylor and M. I. Darby, *Physics of Rare Earth Solids* (Chapman and Hall, London, 1972), p. 114.
[38]I. P. Ipatova and A. V. Subashiev, Zh. Eksp. Teor. Fiz. **66**, 722 (1974) [Sov. Phys.—JETP **39**, 349 (1974)].
[39]S. C. Keeton and T. L. Loucks, Phys. Rev. **168**, 672 (1968).